Lanthanum Chloride Bidirectionally Influences Calcification in Bovine Vascular Smooth Muscle Cells

Wen-Hua Zhao,[1] Bao-Di Gou,[2]* Tian-Lan Zhang,[2] and Kui Wang[2]*

[1] Department of Chemical Biology, Capital Medical University School of Pharmaceutical Sciences, 10 Xitoutiao, You An Men, Beijing 100069, PR China

[2] Department of Chemical Biology, Peking University School of Pharmaceutical Sciences, 38 Xueyuan Road, Beijing 100191, PR China

ABSTRACT

Vascular calcification (VC) is frequent prevalence in patients with chronic kidney disease (CKD) and atherosclerosis. Lanthanum carbonate is used as an orally administered phosphate-binding agent to reduce the gastrointestinal absorption of phosphate and ameliorate VC in advanced CKD. In this study, we used bovine vascular smooth muscle cells as a model VC in vitro and studied the effects of lanthanum chloride on calcium deposition. Exposure of cells to $LaCl_3$ at the concentration of $0.1 \mu M$ suppressed the β-glycerophosphate-induced alkaline phosphatase activity and calcium deposition. Furthermore, $LaCl_3$ upregulated the β-glycerophosphate-suppressed expression of calcium-sensing receptor. In contrast to the inhibitory effect of $LaCl_3$ on calcium deposition, higher level lanthanum ($50 \mu M$) was found to promote immediately precipitation of calcium phosphate in cell culture medium. At this concentration, $LaCl_3$ was found to induce cell apoptosis which involves caspases-9 and -3. These data indicate that the promotory effect of $LaCl_3$ on calcium deposition is likely mediated by induction of apoptosis. Our in vitro findings do suggest that, in the context of raised lanthanum, greater attention should be paid to potential toxic effects associated to the use of lanthanide-based drugs. J. Cell. Biochem. 113: 1776–1786, 2012. © 2011 Wiley Periodicals, Inc.

KEY WORDS: VASCULAR SMOOTH MUSCLE CELLS; LANTHANUM CHLORIDE; CALCIUM PHOSPHATE DEPOSITION; CALCIUM-SENSING RECEPTOR; APOPTOSIS

Vascular calcification (VC) is frequent prevalence in patients with chronic kidney disease (CKD) and atherosclerosis [Doherty, 2004]. It is a pathological process involving medial and intimal calcification, and causes myocardial ischemia and contributes to the morbidity and mortality [Moe and Chen, 2008]. Growing evidence suggests that VC, like bone formation, is an actively regulated process involving both inductive and inhibitory factors. In the advanced CKD population, elevated serum phosphate and increased parathyroid hormone (PTH) levels are likely to be major contributors to VC [Giachelli, 2009]. Thus, phosphate control has become an important therapeutic target with phosphate binders [Hutchison, 2009] and calcimimetics [Saidak et al., 2009; Silver and Naveh-Many, 2009].

Cell apoptosis plays an important role in many pathophysiological conditions and has been recognized as an important mode of cell death in response to cytotoxic treatments. Some studies have shown that vascular smooth muscle cells (VMSCs) are directly responsible for VC [Bennett and Boyle, 1998; Trion and Laarse,

2004; Clarke et al., 2008]. Apoptotic bodies derived from VSMCs may act as nucleating structures for calcium phosphate deposition in the form of hydroxyapatite, so apoptosis is sufficient to precede calcification process [Proudfoot et al., 2000]. Due to the cytotoxic potential of calcium phosphate particles, the crystals have been proved to induce apoptosis in VSMCs [Ewence et al., 2008].

The extracellular calcium-sensing receptor (CaR) belongs to family C of the G-protein-coupled receptors. Extracellular calcium can elicit complex intracellular signals, which plays an important role in regulating mineral ion homeostasis [Hofer and Brown, 2003; Hofer and Lefkimmiatis, 2007; Smajilovic and Tfelt-Hansen, 2007]. Nowadays, it is well-known fact that the CaR is expressed in all the organs and cells that maintain systemic Ca^{2+}. Noteworthy studies have demonstrates that the expression of CaR is reduced in human calcified arteries and in mineralized VSMCs, CaR present in VMSCs may directly prevent mineral deposition [Alam et al., 2009]. Due to its low specificity, cationic lanthanum (La^{3+}), primarily based on its

similarity to Ca^{2+}, also can activate CaR at nanomolar concentration [Carrillo-López et al., 2010].

We have previously reported that $LaCl_3$ suppresses the β-glycerophosphate-induced calcification [Shi et al., 2009]. However, other study found that $50\,\mu M$ $GdCl_3$ can increase the deposition of a mineralized matrix [Alam et al., 2009]. As yet, the exact mechanism of calcification in response to lanthanides is not clearly elucidated. We set out to determine the effects of increased $LaCl_3$ concentrations on in vitro calcification of bovine VSMCs (BVSMCs).

MATERIALS AND METHODS

MATERIALS

Dulbecco's modified Eagle's medium (DMEM), fetal bovine serum (FBS), trypsin, penicillin, and streptomycin were obtained from Gibco BRL (Rockville, MD). Anti-CaR monoclonal antibody was from Affinity Bioreagents (Cambridge, UK). β-actin and the corresponding secondary antibodies were from Cell Signaling (Beverly, MA). NPS2143 was from Tocris Bioscience (Ellisville, MS). Annexin V-FITC Apoptosis detection kit I was obtained from BD Pharmingen (San Diego, CA). Z-VAD-FMK, caspases-3 and -9 activity kit were from Beyotime Institute of Biotechnology (Haimen, China). Unless otherwise indicated, all other reagents, including $LaCl_3$, β-glycerophosphate, Alizarin Red S, MTT, and Rhodamine123 (Rh123) were from Sigma (St. Louis, MO).

VASCULAR SMOOTH MUSCLE CELL CULTURES AND TREATMENT

Bovine vascular smooth muscle cells were isolated from aortic media of bovine by enzymatic isolation according to the method described previously, and cultured in growth medium (DMEM containing 10% FBS, 100 IU/ml penicillin, and 100 mg/ml streptomycin) at $37°C$ in a humidified atmosphere with 5% CO_2. Cells were maintained in growth medium and were used between passages 3 and 8.

After confluence, the cells were then incubated in growth medium or calcification medium (growth medium plus 10 mM β-glycerophosphate) in the presence or absence of $LaCl_3$. The media were replaced every 3 days with fresh one. Full details of culture conditions used in each experiment were specified in the relevant figure legends. Experiments were performed at least three times with triplicate cultures used in every experiment, unless stated otherwise.

ALKALINE PHOSPHATASE ASSAY

Bovine VMSCs were plated in 24-well plates at a density of 5,000 cells/well in growth medium or calcification medium. At the end of the incubation for 9 days, cells were washed three times with PBS, lysed with 1% Triton X-100 in 0.9% NaCl, and then centrifuged. Supernatants were assayed for ALP activity as described previously. ALP values (U/mg) were normalized to protein content that was measured with Bradford assay.

QUANTIFICATION OF CALCIUM DEPOSITION

Bovine VMSCs were plated in 24-well plates at a density of 5,000 cells/well in growth medium or calcification medium. At the end of the incubation for 12 days, calcium deposition was examined

according to the published procedure. Briefly, the cells were decalcified with 0.6 M HCl for 24 h. The calcium content of HCl supernatant was checked by measuring the cell media via inductively coupled plasma–mass spectrometry (HP 7500c, Agilent Technologies, Santa Clara, CA). After decalcification, the cells were washed three times with PBS and solubilized with 0.1 M NaOH/0.1% SDS, and the total protein content was measured with Bradford assay. The calcium content of the cell layer was normalized to cellular protein content.

To visualize the calcified nodules, cells in 12-well plates were washed three times with PBS at day 12, and exposed to Alizarin Red S (2% aqueous) for 5 min at room temperature. After rinsed with PBS, the mineralized nodules were photographed.

WESTERN BLOT ANALYSIS

Western blot analysis was examined according to the published procedure. Briefly, After being washed twice with cold PBS, cells were treated in $250\,\mu l$ of ice-cold lysis buffer (1 mM EGTA, 1 mM dithiothreitol, 300 nM aprotinin, $50\,\mu M$ leupeptin, 1 mM phenyl-methylsulfonyl fluoride, 1 mM sodium vanadate, and 10 mM Tris–HCl pH 7.4) on ice for 10 min, scraped into lysis buffer, and sonicated for 20 s on ice, then were centrifuged at 2,000 rpm at $4°C$ for 10 min. The supernatant were harvested to determine the protein expression of CaR.

The protein concentration of the supernatant was determined using the Bradford protein assay with BSA as standard. Equal amounts of the proteins were subjected to a 10% SDS–PAGE and then the resolved proteins were transferred onto a polyvinylidene difluoride membrane (Immobilon-P, Millipore Corp., Bedford, MA). The membranes were washed with TBST (50 mM Tris–HCl pH 7.5, 150 mM NaCl, and 0.1% Tween-20), blocked with 5% BSA solution in TBST for 1 h at room temperature, and then incubated with anti-CaR monoclonal antibody (1:2,500) in 5% BSA/TBST at $4°C$ overnight. After washing with TBST, the membranes were incubated with horseradish peroxidase-conjugated anti-rabbit antibody diluted 1:2,000 in TBS-T for 1 h at room temperature. After extensive washing, bands were visualized by chemiluminescent method according to the manufacturer's instructions. The optical densities of bands were quantified by Bio-Rad Quantity One 4.6.2 software. β-actin was used at a dilution of 1:400 as a loading control.

MEASUREMENT OF PARTICLE SIZE DISTRIBUTION

The size of the particles in complete cell culture medium and conditional medium with or without various concentrations of $LaCl_3$ was determined with a Zetasizer Nano ZS90 (Malvern Instruments, UK) based on dynamic light scattering at $37°C$. Multiple experimental runs were performed to ensure accuracy. The result was given graphically as a histogram showing particle size distribution.

SCANNING ELECTRON MICROSCOPY AND ENERGY DISPERSIVE X–RAY ANALYSES

Bovine VMSCs were plated in 24-well plates with glass cover slip 4 piece/well at a density of 5,000 cells/well in growth medium. At the end of the incubation for 12 days, cells were washed three times with

PBS and were fixed with step ethanol and osmic acid and then air-dried. The samples were fixed on a polymeric support, and then a thin layer of carbon was sputtered to increase the particles' electrical conductivity, and was submitted to scanning electron microscopy studies and to energy dispersive X-ray microanalysis (Lexica S440i and Supra 55). Microphotographs were recorded, and ratios of Ca/P and La/Ca were checked with the energy X-ray dispersive detector.

CELL VIABILITY ASSAY

BVMSCs were plated in 24-well plates at a density of 5,000 cells/well in growth medium or calcification medium. At the end of the incubation for 12 days, cell viability was measured by assessing mitochondrial activity using MTT assay. MTT in PBS (5 mg/ml) was added to reach a final concentration of 0.5 mg/ml. Further incubation at 37°C for 4 h, the supernatant was removed and the formazan dye dissolved in 150 μl dimethyl sulfoxide. Absorbance in each well was measured at 570 nm on a microplate reader (Multiskan Spectrum, Thermo Electron Corporation). Results are expressed as the percentage of MTT reduction relative to the control cells.

MEASUREMENT OF MITOCHONDRIAL MEMBRANE POTENTIAL

Mitochondrial membrane potential ($\Delta\Psi_m$) was monitored using flow cytometry analysis with rhodamine 123 (Rh123) staining. Briefly, BVMSCs were grown in six-well plates, at the end of the incubation for 12 days, the medium was removed and the treated cells were washed three times in PBS. The cells were stained with Rh123 (10 μM) for 30 min at room temperature in the dark before cell harvesting. The washed cells were resuspended in PBS and the uptake of Rh123 was analyzed using a flow cytometer FACSVantage (SE, Becton Dickinson) with the excitation setting at 488 nm, and signals were acquired at the FL-2 channel. At least 10,000 cells per sample were acquired in histograms and data analyzed by CellQuest software.

Confocal microscope was also used to detect the change of mitochondrial membrane potential in multicellular nodules.

DETECTION OF APOPTOSIS

Apoptosis was evaluated using a flow cytometer with Annexin V-FITC and propidium iodide (PI) staining. Briefly, BVMSCs were grown in six-well plates, at the end of the incubation for 12 days, cells from each sample were suspended in a mixture of 5 μl Annexin V-FITC and 195 μl Annexin V-FITC binding buffer and were then incubated at room temperature for 10 min. The cells were centrifuged at 1,000g for 5 min, suspended again in 190 μl of binding buffer, and then added to with 10 μl of PI working solution. After being filtrated, the samples were analyzed using a flow cytometer FACSVantage. At least 10,000 events were analyzed.

In addition, to get rid of the lysed influence by trypsin, confocal microscope was also used to find out the apoptotic cells morphology in multicellular nodules.

MEASUREMENT OF CASPASE-3 AND CASPASE-9 ACTIVITY

Caspase activities were determined by a colorimetric assay based on the ability of caspases-3, and -9 to change acetyl-Asp-Glu-Val-Asp p-nitroanilide (Ac-DEVD-pNA) and acetyl-Leu-Glu-His-Asp p-nitroanilide (Ac-LEHD-pNA) into a yellow formazan product,

respectively. The absorbance was measured at 405 nm as directed by the caspases-3 and -9 activity assay kit. At the end of the incubation for 12 days, samples were washed three times with PBS, lysed with 1% Triton X-100, and then centrifuged. Sample supernatants containing 50 μg of total protein were added to a reaction buffer containing Ac-DEVD-pNA (2 mM) or Ac-LEHD-pNA (2 mM), incubated for 4 h at 37°C, and then the absorbance of yellow pNA was measured by a spectrometer at 405 nm. The specific caspase-3 or -9 activity was normalized for total protein measured according to Bradford method.

CASPASE INHIBITION STUDIES

Bovine VSMCs were plated at a density of 5,000 cells/well in growth medium or calcification medium in 24-well plates. With or without pretreatment with 20 μM Z-VAD-FMK for 1 h as described in the figure legends, cells were incubated in the absence or presence of LaCl₃. At the end of the incubation for 12 days, cells were collected and washed twice with chilled PBS, calcium deposition was examined according to the quantification of calcium deposition procedure.

STATISTICAL ANALYSIS

Data shown are mean ± standard deviation (SD) from 2 to 4 separate experiments each performed in quadruplicate or triplicate. Significance was determined using one-way analysis of variance. $P < 0.05$ was considered significant.

RESULTS

EFFECT OF LaCl₃ ON β-GLYCEROPHOSPHATE-INDUCED CALCIFICATION IN BVMSCs

The addition of β-glycerophosphate to the culture medium induces osteoblastic differentiation and mineral deposition in BVMSCs. In this study, cells showed a marked increase in ALP activity and calcium content when incubated with calcification medium (Fig. 1A,B). Calcification was assessed by alizarin red staining, cells did not calcify when cultured in growth medium without β-glycerophosphate (Fig. 1C). Interestingly, we observed that LaCl₃ played a dual effect on β-glycerophosphate-induced calcification: lower concentrations of lanthanum (0.1 μM) led to a significant reduction of ALP activity and calcium content compared to β-glycerophosphate alone, but higher concentration of lanthanum (50 μM) showed a stimulative role (Fig. 1).

EFFECT OF LaCl₃ ON EXPRESSION OF CAR IN BVMSCs

CaR downregulation has been shown to be involved in the process of calcification of BVMSCs. We observed that β-glycerophosphate could lead to an ∼5-fold downregulation of CaR expression relative to the non-calcification control, and this decrease was blocked with 0.1 μM LaCl₃ (Fig. 2A,B). Upon pretreating cells with NPS2143, a CaR antagonist, the inhibitory effect of 0.1 μM LaCl₃ on β-glycerophosphate-induced calcification was abolished (Fig. 2C). These results imply that the significance of CaR in mediating the effect of LaCl₃. Although 50 μM LaCl₃ increased β-glycerophosphate-induced calcification, a further β-glycerophosphate-induced decrease in CaR expression was not observed.
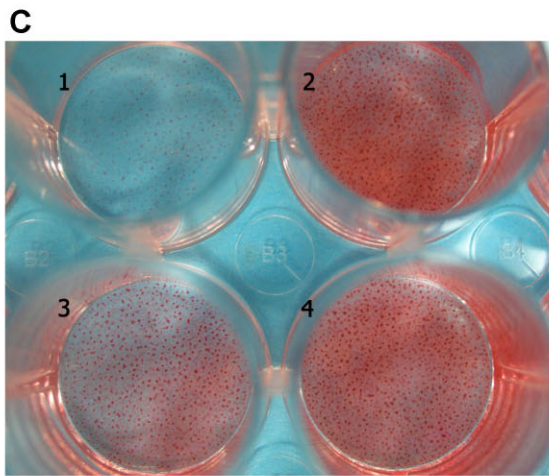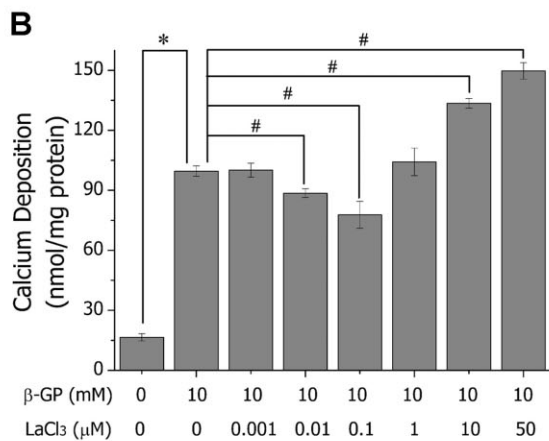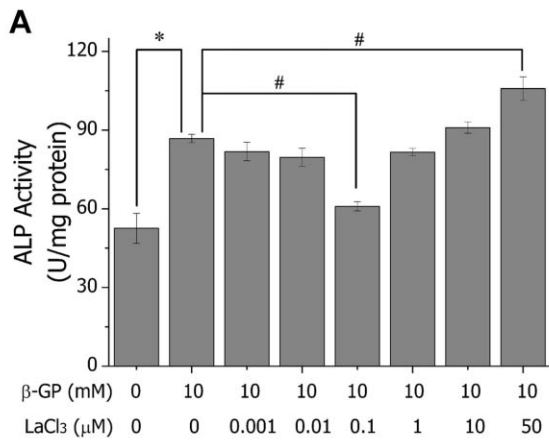
Fig. 1. Effect of LaCl$_3$ on β–glycerophosphate–induced ALP activity and calcium deposition in bovine VMSCs. Cells were incubated in growth medium and calcification medium in the absence or presence of the indicated concentration of LaCl$_3$. ALP activity (A) and calcium deposition (B) were determined with cells after treatment for 9 and 12 days, respectively. Both are normalized to cellular protein content. Data are presented as mean ± SD from a representative of three separate experiments performed in quadruplicate. *$P < 0.05$ versus non-calcification control; #$P < 0.05$ versus LaCl$_3$-free calcification control. C: Photograph of mineralized nodules at day 12 stained with Alizarin Red S. 1: Non-calcification control; 2: 50 μM LaCl$_3$ + 10 mM β-GP; 3: 0.1 μM LaCl$_3$ + 10 mM β-GP; 4: LaCl$_3$-free calcification control. [Color figure can be seen in the online version of this article, available at http://wileyonlinelibrary.com/journal/jcb]
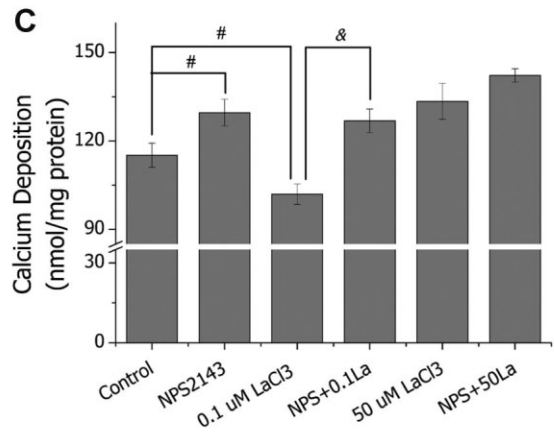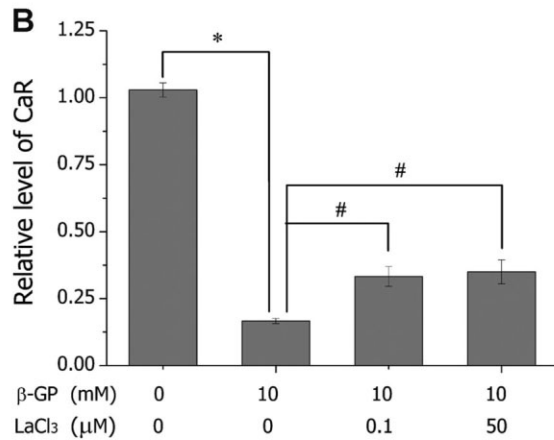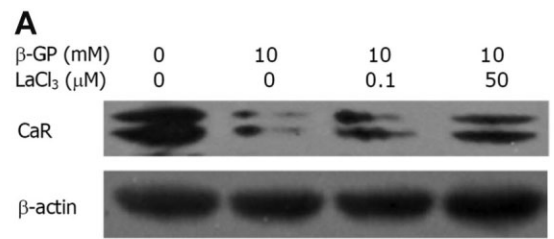

Fig. 2. Effect of LaCl$_3$ on β–glycerophosphate–induced expression of CaR in bovine VSMCs. Cells were incubated for 12 days under growing and calcifying conditions in the absence or presence of the indicated concentration of LaCl3. A: CaR protein was detected by Western blotting in total lysates after 12 days. B: the data on O.D. (% of control) are presented as mean ± SD (n = 3). Typical Western blot detections are shown at the bottoms of bar graphics. *$P < 0.05$ versus non-calcification control, #$P < 0.05$ versus LaCl$_3$-free calcification control. C: After pretreatment with 0.1 ng/ml NPS-2143 for 1 day, cells were incubated in the calcification medium in the absence or presence of the indicated concentration of LaCl$_3$ for 12 days. Calcium deposition was measured, and data are presented as mean ± SD from a representative of three separate experiments performed in quadruplicate. #$P < 0.05$ versus LaCl$_3$-free calcification control; &$P < 0.05$ versus LaCl$_3$-containing calcification control.

EFFECT OF LaCl$_3$ ON MORPHOLOGY AND COMPOSITION OF PRECIPITATES IN BVMSCs

Some population of BVMSCs grow into multicellular nodules, the matrix of which became calcified. Under calcification conditions, cells grouped into multicellular aggregates or nodules (Fig. 3).
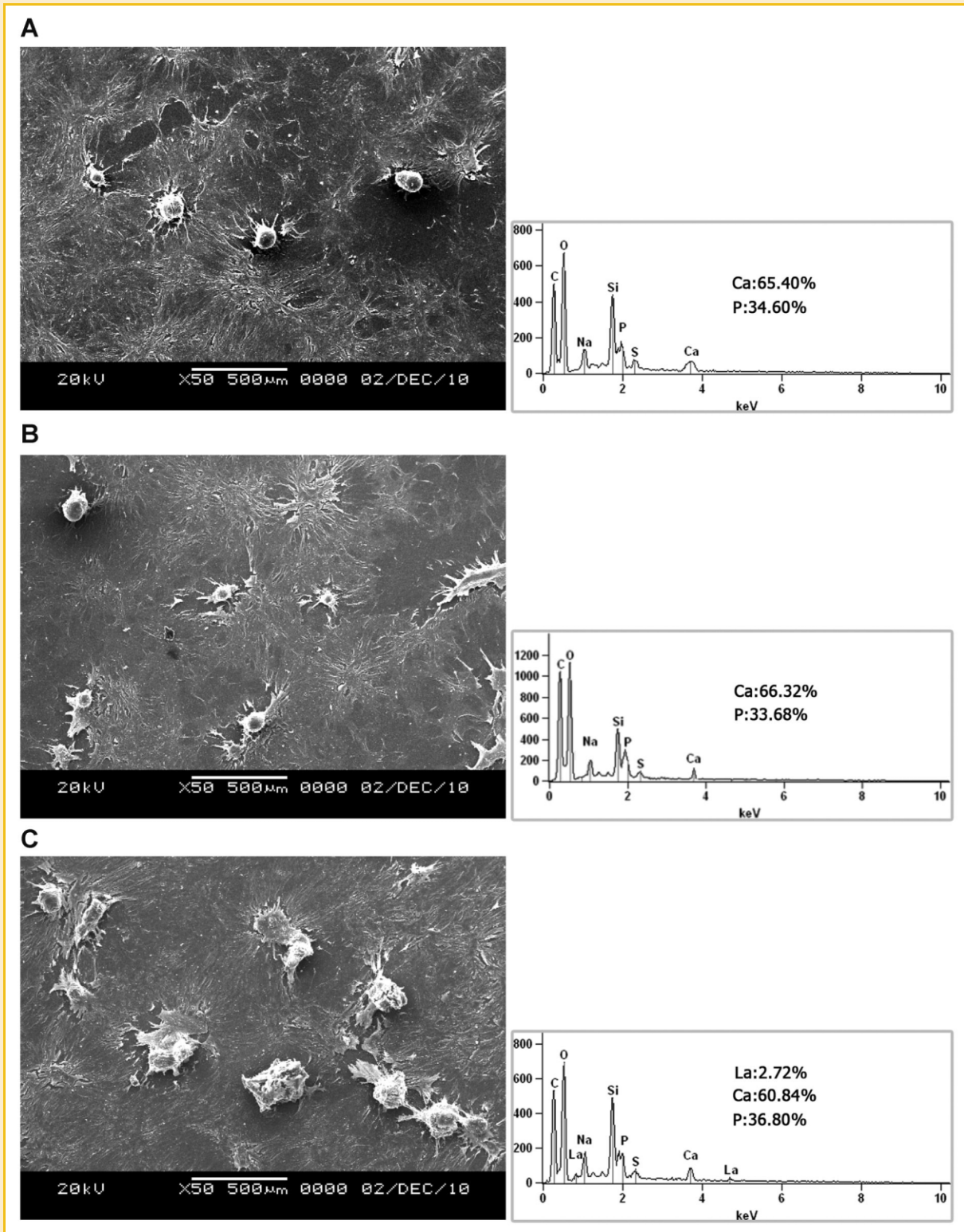
Fig. 3. Scanning electron micrographs of precipitates formed in multicellular nodules under calcifying conditions. A: LaCl$_3$-free calcification control; B: 0.1 μM LaCl$_3$ + 10 mM β-GP; C: 50 μM LaCl$_3$ + 10 mM β-GP. Scale bars are noted in each panel, and elemental compositions of precipitates are analyzed by energy dispersive X-ray analysis, respectively.
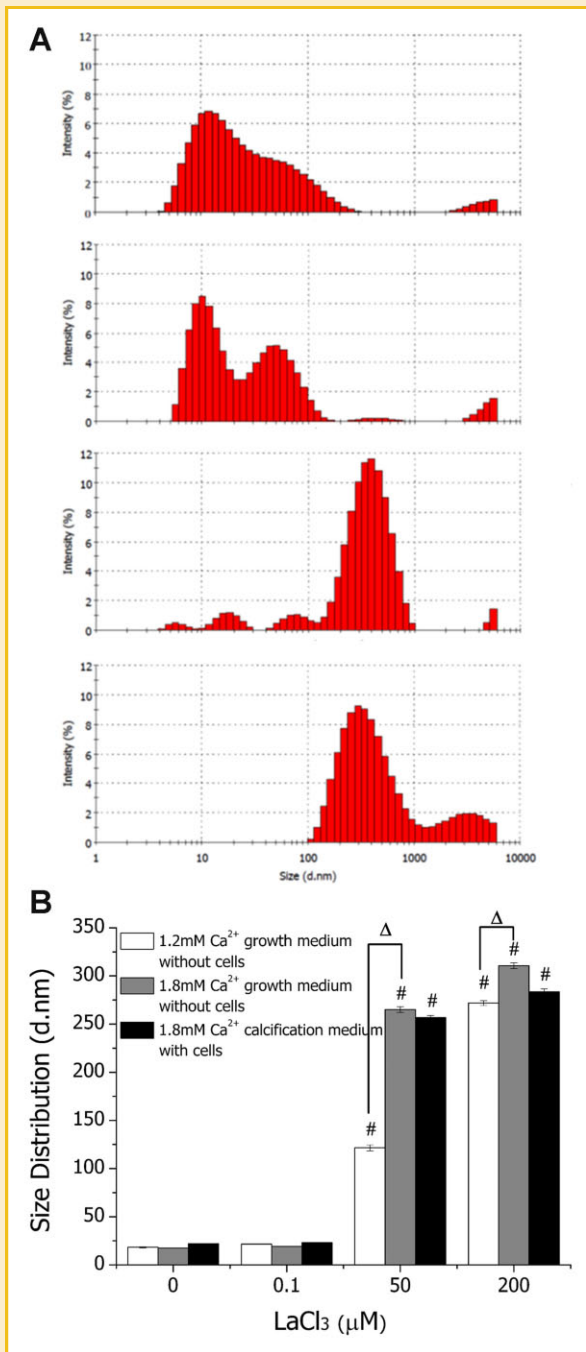
Fig. 4. Effect of LaCl₃ on size distribution of precipitates in cell culture medium. A: Particle size distributions in growth medium. From the top down, concentrations of LaCl₃ are 0, 0.1, 50, and 200 μM. B: Particle size distributions in growth medium containing 1.2 mM Ca²⁺ (white columns), 1.8 mM Ca²⁺ (gray columns), and calcification medium incubation with cells (black columns). #$P < 0.05$ versus LaCl₃-free control; Δ$P < 0.05$ versus medium with 1.2 mM Ca²⁺. [Color figure can be seen in the online version of this article, available at http://wileyonlinelibrary.com/journal/jcb]

Electron microscopic and energy dispersive X-ray analysis of nodules showed that they consisted of mostly calcium, phosphorous, and oxygen, consistent with an apatite-like material. In the presence of 50 μM LaCl₃, VMSCs formed more and bigger nodules in which
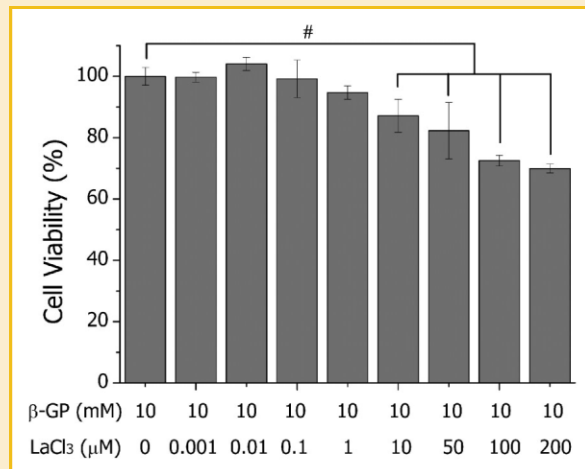

Fig. 5. Effect of LaCl₃ on the cell viability in bovine VMSCs. Cells were incubated for 12 days under calcifying conditions in the absence or presence of the indicated concentration of LaCl₃. Cell viability was examined by MTT assay, and data are presented as mean ± SD of three separate experiments performed in quadruplicate. #$P < 0.05$ versus LaCl₃-free calcification control.

were confirmed the coexistence of lanthanum, calcium, and phosphorus by elemental analysis (Fig. 3C).

EFFECT OF LaCl₃ ON SIZE DISTRIBUTION OF PRECIPITATES IN CULTURE MEDIUM

Culture medium is a metastable calcium phosphate system. In this study, dynamic light scattering experiments were carried out for detection of a scattered intensity of particles in the solutions. Figure 4A shows typical profiles of particle size distribution in culture medium. The new peak on the right side is caused by addition of LaCl₃, showing larger size and higher intensity with increasing concentration of LaCl₃. Moreover, the size distributions of precipitates increase with the supply amount of Ca²⁺ (Fig. 4B). In addition, the size distribution of these particles ranges from 100 to 400 nm in cell culture medium. These results confirmed the promotory effect of La³⁺ on calcium precipitation, and the majority of the observed precipitates was calcium phosphate.

EFFECT OF LaCl₃ ON CELL VIABILITY IN BVMSCs

Calcium phosphate particles exhibit a cytotoxic potential. To determine the promotion in calcification was due to the reduction in cell viability, the effects of LaCl₃ on cytotoxicity were investigated with an MTT assay. As shown in Figure 5, lower concentration of lanthanum (0.001–1 μM) did not reduce cell viability in the presence of β-glycerophosphate, but the exposure to higher LaCl₃ (10–200 μM) caused a significant decrease in VMSC viability in a concentration-dependent way.

EFFECT OF LaCl₃ ON MITOCHONDRIAL MEMBRANE POTENTIAL IN BVMSCs

Mitochondrial depolarization is considered as an irreversible step in the apoptosis process. Consequently, we have made an attempt to measure the loss of mitochondrial membrane potential ($\Delta\Psi_m$) using

a fluorogenic probe Rh123. As shown in confocal imaging, lower fluorescence in the presence 50 μM LaCl$_3$ indicates significantly greater loss of mitochondrial membrane potential in multicellular nodules compared to the LaCl$_3$-free calcified individuals (Fig. 6C). A concentration-dependent decrease in $\Delta\Psi_m$ after exposure to higher concentration of LaCl$_3$ (50–200 μM) was also observed (Fig. 6D). In addition, 0.1 μM of LaCl$_3$ did not affect the level of fluorescence compared to the LaCl$_3$-free calcified individuals (Fig. 6B).

EFFECT OF LaCl$_3$ ON CELL APOPTOSIS IN BVMSCs

Apoptosis precedes VMSCs calcification and apoptotic bodies may act as nucleating structures for calcium crystal formation. To find out whether apoptosis occurred in BVMSCs nodules, Annexin V-FITC and PI were used to visualize apoptotic cells. As shown in

Figure 7, a 12-day incubation with higher concentration of LaCl$_3$ (50 μM) led to an increase in both apoptosis (Annexin V-FITC positive) and necrosis (PI positive). Flow cytometer analysis also showed that LaCl$_3$ (50–200 μM) markedly increase apoptotic index (Fig. 7D). However, after 0.1 μM of LaCl$_3$ treatment, apoptotic and necrotic cells in nodules were decreased compared to the LaCl$_3$-free calcified individuals (Fig. 7B).

EFFECT OF LaCl$_3$ ON CASPASE ACTIVITIES IN BVMSCs

The central component of apoptosis is a family of caspases which are responsible for triggering and affecting the apoptotic process. To ascertain whether the effect of LaCl$_3$ resulted from regulating caspase activity, we measured caspases-9 and -3 catalytic activity using specific chromogenic substrates. Treatment of cells with
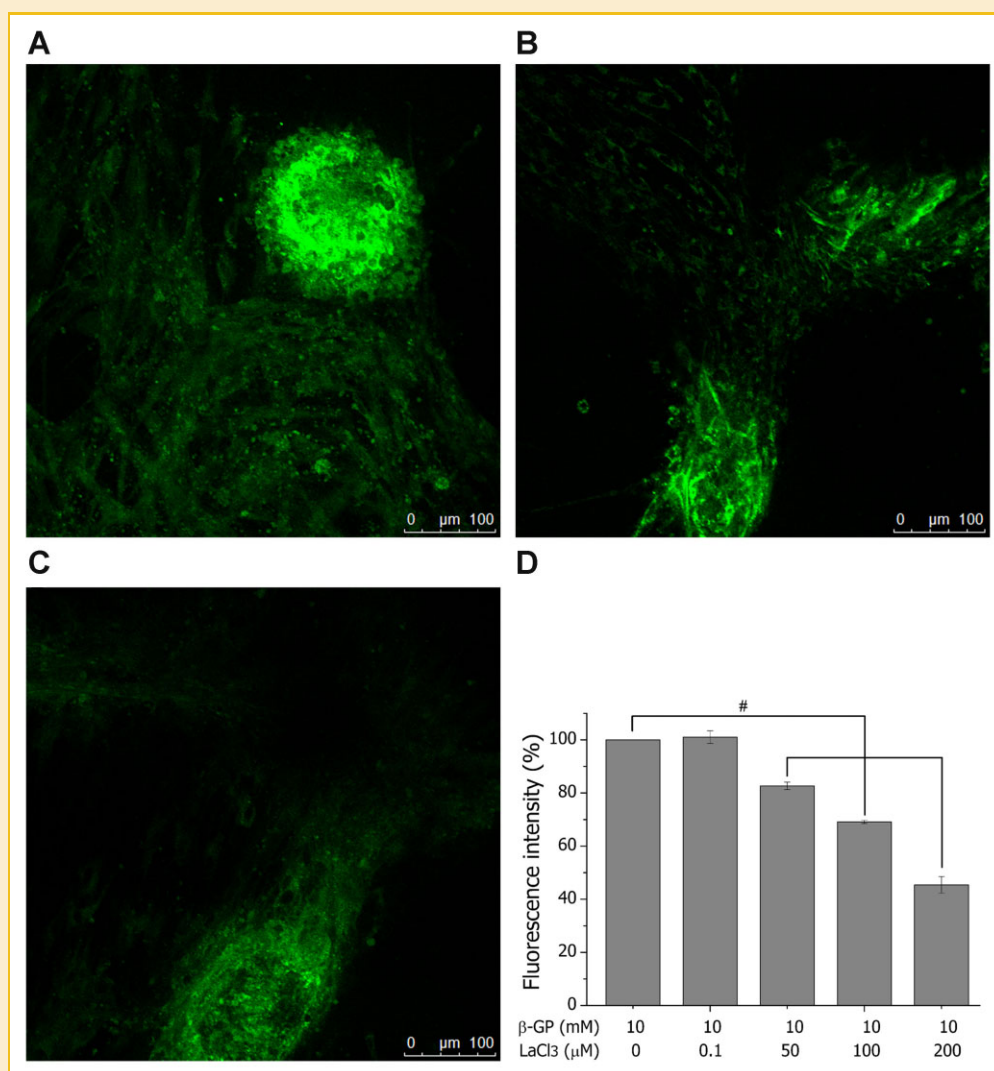

Fig. 6. Effect of LaCl$_3$ on mitochondrial membrane potential in bovine VMSCs. Cells were incubated under calcifying conditions in the absence or presence of the indicated concentration of LaCl$_3$ for 12 days, and cells were stained with fluorescent probe Rh123. Fluorescence alteration in multicellular nodules was determined by confocal microscopy, and the picture is representative of one of the three similar results. A: LaCl$_3$–free calcification control; B: 0.1 μM LaCl$_3$ + 10 mM β–GP; C: 50 μM LaCl$_3$ + 10 mM β–GP. D: Fluorescence intensity was analyzed using flow cytometer, and data are presented as mean ± SD from three separate experiments. #$P < 0.05$ versus LaCl$_3$–free calcification control. [Color figure can be seen in the online version of this article, available at http://wileyonlinelibrary.com/journal/jcb]
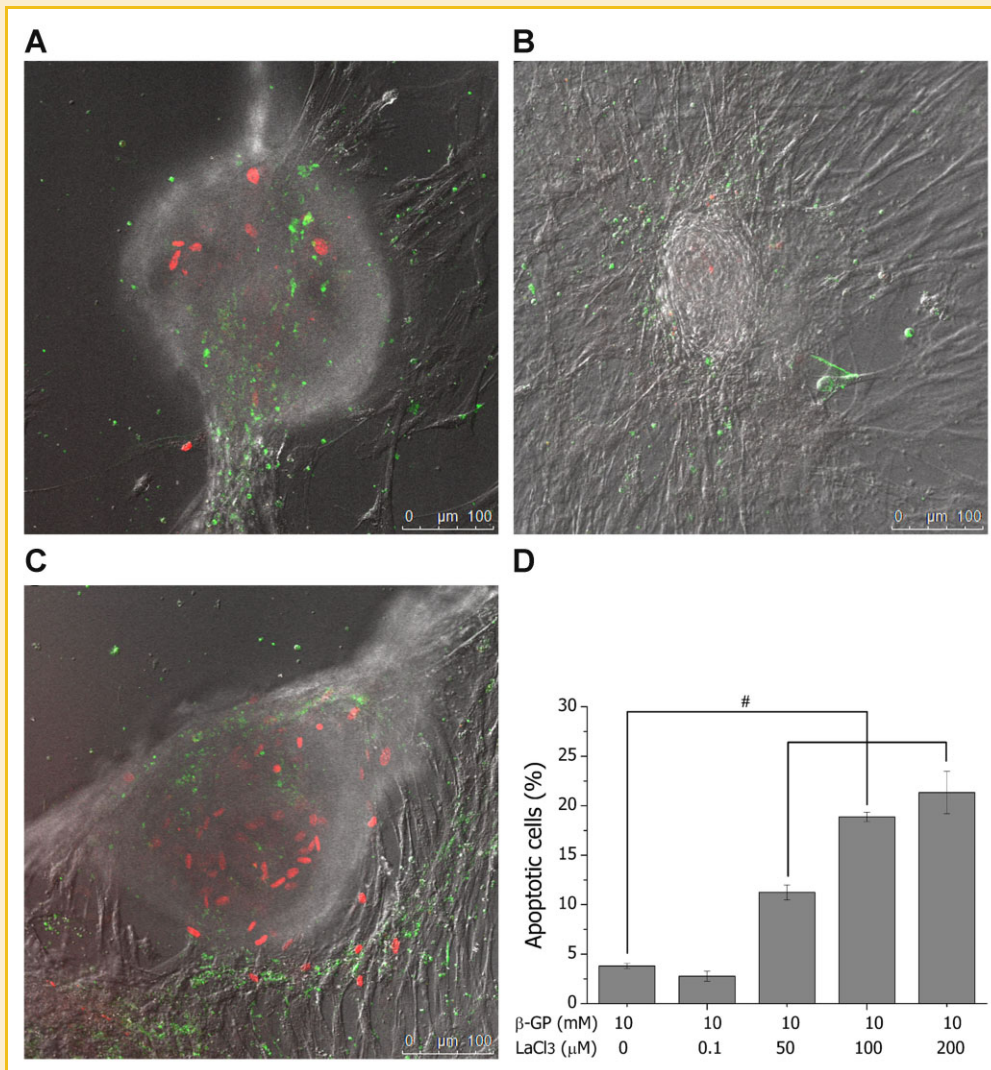
Fig. 7. Effect of LaCl$_3$ on cell apoptosis in bovine VMSCs. Cells were incubated under calcifying conditions in the absence or presence of the indicated concentration of LaCl$_3$ for 12 days, and cells were stained with fluorescent probe annexin-V FITC and PI. Fluorescence alteration in multicellular nodules was determined by confocal microscopy, and the picture is representative of one of the three similar results. A: LaCl$_3$-free calcification control; B: 0.1 μM LaCl$_3$ + 10 mM β-GP; C: 50 μM LaCl$_3$ + 10 mM β-GP. D: The percentage of apoptosis was analyzed using flow cytometer, and data are presented as mean ± SD from three separate experiments. #$P < 0.05$ versus LaCl$_3$-free calcification control. [Color figure can be seen in the online version of this article, available at http://wileyonlinelibrary.com/journal/jcb]

50 μM LaCl$_3$ caused caspases-9 and -3 activity increase in the presence and absence of β-glycerophosphate (Fig. 8A,B). The effects of LaCl$_3$ on apoptosis are not only stimulatory but also inhibitory, as shown in Figure 8B, 0.1 μM LaCl$_3$ decreased significantly β-glycerophosphate-induced caspase-3 activity. In the presence of a pan-caspase inhibitor, Z-VAD-FMK, LaCl$_3$-promoted calcification was completely blocked through 1 h pretreatment with a (Fig. 8C). These results indicate caspases-9 and -3 were involved in apoptosis induced by higher concentration lanthanum in BVSMCS.

DISCUSSION

Recently, some gadolinium-based contrast agents (GBCAs) has been related with nephrogenic systemic fibrosis [Rofsky et al., 2008;

Sanyal et al., 2011]. Lanthanum and gadolinium are close in the periodic table and have analog physiochemical properties. The use of lanthanum carbonate (Fosrenol®) as an oral phosphate binder might have some analogies [Aime et al., 2007; Brambilla et al., 2008; Broe, 2008]. Although lanthanum carbonate is apparently safe for patients with advanced CKD, some clinic reports have shown that lanthanum therapy is possibly responsible for acute liver failure [Leeuw et al., 2008] and encephalopathy [Fraile et al., 2011]. Clearly, more work appears necessary to assess potential toxic effects associated to the use of lanthanum-based drugs.

Lower lanthanum level suppresses the calcification via upregulating decreased CaR expression in BVSMCs. The CaR senses alterations in the level of extracellular calcium and responds with changes in function. The study by Alam et al. [2009] strongly suggest that a functional CaR is necessary to maintain a VMSCs
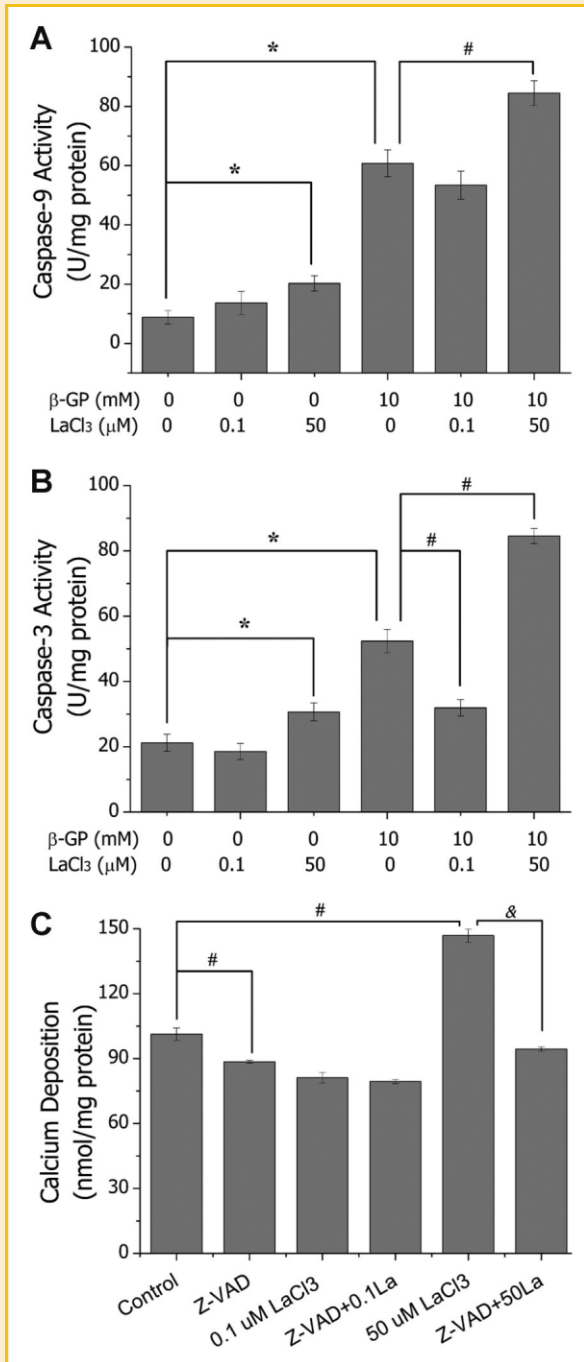
Fig. 8. Effect of LaCl₃ on enzyme activities of caspase–3 (A) and caspase–9 (B) in bovine VSMCs. Cells were incubated for 12 days under growing and calcifying conditions in the absence or presence of the indicated concentration of LaCl₃, caspase activity was determined by a colorimetric assay. Bar graph indicates the mean ± SD (n = 4). *P < 0.05 versus non–calcification control, #P < 0.05 versus LaCl₃–free calcification control. C: After pretreatment with 20 μM Z–VAD–FMK for 1 h, cells were incubated in the calcification medium in the absence or presence of the indicated concentration of LaCl₃ for 12 days. Calcium deposition was measured, and data are presented as mean ± SD from a representative of three separate experiments performed in quadruplicate. #P < 0.05 versus LaCl₃–free calcification control; &P < 0.05 versus LaCl₃–containing calcification control.

phenotype and to keep calcification suppressed. Moreover, it is shown that the stimulation of CaR with calcimimetics attenuates VMSCs calcification [Mizobuchi et al., 2004]. Since lanthanum has higher binding affinity than calcium, it can act as a substitute or antagonist for calcium or as a calcium channel blocker to explain many of the known biological effects of calcium [Kramsch et al., 1980]. The nanomolar LaCl₃ has been found to activate the CaR and enhanced CaR sensitivity to calcium [Carrillo-López et al., 2010]. In our study, VMSCs treated with 0.1 μM LaCl₃ showed ameliorated calcium deposition in extracellular matrix in the presence of β-glycerophosphate. In addition, the level of CaR expression downregulated by β-glycerophosphate was increased. In our previous study, we have found that pretreatment with pertussis toxin (PTx), a Gi protein inhibitor, suppressed the LaCl₃-induced osteoblastic differentiation in rat VMSCs [Shi et al., 2009]. Taken together, these results indicate that the significance of CaR in mediating the effect of LaCl₃ on inhibiting VMSCs calcification. Lanthanum carbonate is an effective and beneficial phosphate-binding agent [Freitas et al., 2007; Hutchison, 2009]; in addition, other modes of action exist. Supporting this point, a recent animal study has found that lanthanum content was elevated in aortas with VC after administration of lanthanum acetate [Zhou et al., 2009]. Moreover, lanthanum appears to exert its vascular effects via changes in oxidative stress or bone remodeling [Nikolov et al., 2011]. In addition, the level of PTH decreased after the use of lanthanum carbonate compared with sevelamer-HCl [Hutchison and Laville, 2008; Navaneethan et al., 2009]. Due to the low systemic absorption (0.0013%), serum lanthanum levels is <0.2 nM in health human subjects [Pennick et al., 2006]. However, lanthanum exposure could raise the level to 0.1 μM (13.9 ng/ml) at certain circumstances [Hutchison et al., 2008]. Therefore, the roles of lanthanum observed in the present study could be relevant to that happens in vivo.

Higher lanthanum level enhances the calcification via calcium phosphate particles via inducing apoptosis in BVSMCs. Under the same condition, 50 μM LaCl₃ also upregulated decreased CaR expression similar to 0.1 μM group. However, higher concentration of lanthanum was surprisingly found to promote VMSCs calcification. To explain the reason for the different action pattern, we further found that the lanthanum coexisted with calcium and phosphorus in multicellular nodules. VMSCs were maintained in DMEM medium containing 1.8 mM calcium chloride and 0.9 mM sodium phosphate monobasic, being a metastable calcium phosphate solution [Jonge et al., 2009; Mandel and Tas, 2010]. After adding lanthanum solution into the cell medium at higher concentrations, we observed white cloudy substance on the bottom of culture plates, and identified particulate matter with lanthanum-containing calcium phosphate precipitation. Indeed, calcium phosphate particles are prevailing in humans and have been shown to have biological activities in many cell types [Motskin et al., 2009; Sommer, 2010; Yuan et al., 2010]. In a recent study, this has been shown that synthetic calcium phosphate crystals and human atherosclerosis-derived crystals induced cell apoptosis in human VMSCs with their potency depending on their size [Ewence et al., 2008]. It is well-known that apoptosis precedes VSMC calcification and apoptotic bodies derived from VSMCs may act as nucleating

structures for deposition of calcium phosphate mineral [Proudfoot et al., 2000]. The exposure to $50\,\mu M$ $LaCl_3$ reduced cell viability, decreased mitochondrial membrane potential, and induced cell apoptosis involving caspases-9 and -3. These facts indicate that higher lanthanum level is likely to have a pro-apoptotic potential and thereby enhance calcification. At the higher concentration of $LaCl_3$, a part of lanthanum ions are in the "free" form [Kubota et al., 2000], which could upregulate the CaR expression and, at the same time, it is likely to block calcium channels preventing calcium influx. Other studies previously found the role of lanthanum in promoting calcification was also demonstrated in vivo. For example, rats underwent local calcification when injected $LaCl_3$ into the subcutaneous tissue [Garrett and McClure, 1981], while intravenous injections produced a milieu proven to be conducive to the deposition of calcium phosphate [Johannsson et al., 1968]. Indeed, there is continuing concern regarding the possibility of metal accumulation in tissues over time and possible long-term side effects. In fact, in particular in patients, some reports have suggested this possibility [Lacour et al., 2005; Davis and Abraham, 2009].

In conclusion, our studies have shown for the first time that $LaCl_3$ bidirectionally influences calcification in BVMSCs: lower $LaCl_3$ level suppressed the calcification via upregulating decreased CaR expression; higher $LaCl_3$ level promoted precipitation of calcium phosphate, and these lanthanum-containing calcium phosphate particles induced cell apoptosis and enhanced calcification.

REFERENCES

Aime S, Canavese C, Stratta P. 2007. Advisory about gadolinium calls for caution in the treatment of uremic patients with lanthanum carbonate. Kidney Int 72:1162–1163.

Alam M, Kirton JP, Wilkinson FL, Towers E, Sinha S, Rouhi M, Vizard TN, Sage AP, Martin D, Ward DT, Alexander MY, Riccardi D, Canfield AE. 2009. Calcification is associated with loss of functional calcium-sensing receptor in vascular smooth muscle cells. Cardiovasc Res 81:260–268.

Bennett MR, Boyle JJ. 1998. Apoptosis of vascular smooth muscle cells in atherosclerosis. Atherosclerosis 138:3–9.

Brambilla S, Valaperta S, Graziani G, Montanelli A. 2008. Gadolinium and lanthanum: A iatrogenic transmetallation. Clin Biochem 41:1029–1033.

Broe MED. 2008. Can the risk of gadolinium be extrapolated to lanthanum. Semin Dial 21:142–144.

Carrillo-López N, Fernández-Martín JL, Álvarez-Hernández D, González-Suárez I, Castro-Santos P, Román-García P, López-Novoa JM, Cannata-Andía JB. 2010. Lanthanum activates calcium-sensing receptor and enhances sensitivity to calcium. Nephrol Dial Transplant 25:2930–2937.

Clarke MCH, Littlewood TD, Figg N, Maguire JJ, Davenport AP, Goddard M, Bennett MR. 2008. Chronic apoptosis of vascular smooth muscle cells accelerates atherosclerosis and promotes calcification and medial degeneration. Circ Res 102:1529–1538.

Davis RL, Abraham JL. 2009. Lanthanum deposition in a dialysis patient. Nephrol Dial Transplant 24:3247–3250.

Doherty TM. 2004. Molecular, endocrine, and genetic mechanisms of arterial calcification. Endocr Rev 25:629–672.

Ewence AE, Bootman M, Roderick HL, Skepper JN, McCarthy G, Epple M, Neumann M, Shanahan CM, Proudfoot D. 2008. Calcium phosphate crystals induce cell death in human vascular smooth muscle cells: A potential mechanism in atherosclerotic plaque destabilization. Circ Res 103:e28–e34.

Fraile P, Cacharro LM, Garcia-Cosmes P, Rosado C, Tabernero aJM. 2011. Encephalopathy caused by lanthanum carbonate. NDT Plus 4:192–194.

Freitas DD, Donne RL, Hutchison AJ. 2007. Lanthanum carbonate—A first line phosphate binder? Semin Dial 20:325–328.

Garrett IR, McClure J. 1981. Lanthanide-induced calcergy. J Pathol 135:267–275.

Giachelli CM. 2009. The emerging role of phosphate in vascular calcification. Kidney Int 75:890–897.

Hofer MA, Brown EM. 2003. Extracellular calcium sensing and signalling. Nat Rev Mol Cell Biol 4:530–538.

Hofer AM, Lefkimmiatis K. 2007. Extracellular calcium and cAMP: Second messengers as "third messengers"? Physiology 22:320–327.

Hutchison AJ. 2009. Oral phosphate binders. Kidney Int 75:906–914.

Hutchison AJ, Laville M. 2008. Switching to lanthanum carbonate monotherapy provides effective phosphate control with a low tablet burden. Nephrol Dial Transplant 23:3677–3684.

Hutchison AJ, Barnett E, Krause R, Kwan JTC, Siami GA. 2008. Long-term efficacy and safety profile of lanthanum carbonate: Results for up to 6 years of treatment. Nephron Clin Pract 110:c15–c23.

Johannsson Perrault G, Savoie L, Tuchweber B. 1968. Action of various metallic chlorides on calcaemia and phosphataemia. Br J Pharm Chemother 33:91–97.

Jonge LTd, Beucken JJJPvd, Leeuwenburgh SCG, Hamers AAJ, Wolke JGC, Jansen JA. 2009. In vitro responses to electrosprayed alkaline phosphatase/calcium phosphate composite coatings. Acta Biomater 5:2773–2782.

Kramsch DM, Aspen AJ, Apstein CS, Memorial E. 1980. Suppression of experimental atherosclerosis by the Ca++-antagonist lanthanum. J Clin Invest 65:967–981.

Kubota Y, Takahashi S, Takahashi I, Patrick G. 2000. Different cytotoxic response to gadolinium between mouse and rat alveolar macrophages. Toxicol In Vitro 14:309–319.

Lacour B, Lucas A, Auchère D, Ruellan N, Patey NMDS, Drüeke TB. 2005. Chronic renal failure is associated with increased tissue deposition of lanthanum after 28-day oral administration. Kidney Int 67:1062–1069.

Leeuw KD, Woestenburg A, Verbeelen D. 2008. Lanthanum carbonate possibly responsible for acute liver failure in a patient with Child–Pugh stage A liver cirrhosis. NDT Plus 6:412–413.

Mandel S, Tas AC. 2010. Brushite ($CaHPO_4\cdot 2H_2O$) to octacalcium phosphate ($Ca_8(HPO_4)_2(PO_4)_4\cdot 5H_2O$) transformation in DMEM solutions at $36.5°C$. Mater Sci Eng C 30:245–254.

Mizobuchi M, Hatamura I, Ogata H, Saji F, Uda S, Shiizaki K, Sakaguchi T, Negi S, Kinugasa E, Koshikawa S, Akizawa T. 2004. Calcimimetic compound upregulates decreased calcium-sensing receptor expression level in parathyroid glands of rats with chronic renal insufficiency. J Am Soc Nephrol 15:2579–2587.

Moe SM, Chen NX. 2008. Mechanisms of vascular calcification in chronic kidney disease. J Am Soc Nephrol 19:213–216.

Motskin M, Wright DM, Muller K, Kyle N, Gard TG, Porter AE, Skepper JN. 2009. Hydroxyapatite nano and microparticles: Correlation of particle properties with cytotoxicity and biostability. Biomaterials 30:3307–3317.

Navaneethan SD, Palmer SC, Craig JC, Elder GJ, Strippoli GFM. 2009. Benefits and harms of phosphate binders in CKD: A systematic review of randomized controlled trials. Am J Kidney Dis 54:619–637.

Nikolov IG, Joki N, Nguyen-Khoa T, Guerrera IC, Maizel J, Benchitrit J, Reis LMd, Edelman A, Lacour B, Jorgetti V, Drüeke TB, Massy ZA. 2011. Lanthanum carbonate, like sevelamer-HCl, retards the progression of vascular calcification and atherosclerosis in uremic apolipoprotein E-deficient mice. Nephrol Dial Transplant DOI: 10.1093/ndt/gfr254.

Pennick M, Dennis K, Damment SJP. 2006. Absolute bioavailability and disposition of lanthanum in healthy human subjects administered lanthanum carbonate. J Clin Pharmacol 46:738–746.

Proudfoot D, Skepper JN, Hegyi L, Bennett MR, Shanahan CM, Weissberg PL. 2000. Apoptosis regulates human vascular calcification in vitro: Evidence for Initiation of vascular calcification by apoptotic bodies. Circ Res 87:1055–1062.

Rofsky NM, Sherry AD, Lenkinski RE. 2008. Nephrogenic systemic fibrosis: A chemical perspective. Radiology 247:608–612.

Saidak Z, Brazier M, Kamel S, Mentaverri R. 2009. Agonists and allosteric modulators of the calcium-sensing receptor and their therapeutic applications. Mol Pharmacol 761:1144–2009.

Sanyal S, Marckmann P, Scherer S, Abraham JL. 2011. Multiorgan gadolinium (Gd) deposition and fibrosis in a patient with nephrogenic systemic fibrosis—An autopsy-based review. Nephrol Dial Transplant 26:3616–3626.

Shi Y-L, Wang L-W, Huang J, Gou B-D, Zhang T-L, Wang K. 2009. Lanthanum suppresses osteoblastic differentiation via pertussis Toxin-sensitive G protein signaling in rat vascular smooth muscle cells. J Cell Biochem 108:1184–1191.

Silver J, Naveh-Many T. 2009. Phosphate and the parathyroid. Kidney Int 75:898–906.

Smajilovic S, Tfelt-Hansen J. 2007. Calcium acts as a first messenger through the calcium-sensing receptor in the cardiovascular system. Cardiovasc Res 75:457–467.

Sommer AP. 2010. Cytotoxicity of calcium phosphate crystals and human-derived nanoparticles: An overlooked link. Circ Res 106:e10.

Trion A, Laarse Avd. 2004. Vascular smooth muscle cells and calcification in atherosclerosis. Am Heart J 147:808–814.

Yuan Y, Liu C, Qian J, Wang J, Zhang Y. 2010. Size-mediated cytotoxicity and apoptosis of hydroxyapatite nanoparticles in human hepatoma HepG2 cells. Biomaterials 31:730–740.

Zhou Y-B, Jin S-J, Cai Y, Teng X, Chen L, Tang C-S, Qi Y-F. 2009. Lanthanum acetate inhibits vascular calcification induced by vitamin D3 plus nicotine in rats. Exp Biol Med 234:908–917.